Available online at www.sciencedirect.com
ScienceDirect
Journal of Nuclear Materials 367–370 (2007) 1487–1491
journal of nuclear materials
www.elsevier.com/locate/jnucmat

Hydrogen retention properties of co-deposition under high-density plasmas in TRIAM-1M

M. Tokitani [a,*], M. Miyamoto [b], K. Tokunaga [c], T. Fujiwara [c], N. Yoshida [c], M. Sakamoto [c], H. Zushi [c], K. Hanada [c] TRIAM Group [c], S. Nagata [d], B. Tsuchiya [d]

[a] *Interdisciplinary Graduate School of Engineering Sciences, Kyushu University, Kasuga, Fukuoka 816-8580, Japan*
[b] *Department of Material Science, Shimane University, Matsue, Shimane 690-8504, Japan*
[c] *Research Institute for Applied Mechanics, Kyushu University, Kasuga, Fukuoka 816-8580, Japan*
[d] *Institute for Materials Research, Tohoku University, Sendai, Miyagi 980-8577, Japan*

Abstract

Retention of hydrogen in co-deposits formed under high-density plasma discharge in TRIAM-1M was studied. In order to quantify the retained hydrogen, material probe experiments were performed under the high-density ($\tilde{n}_e \sim 10^{19}$ m^{-3}) discharges. After the exposure to the plasma, the quantitative analysis of deposition, hydrogen retention, and microscopic modification of specimens were performed by means of ion beam analysis and transmission electron microscopy. The co-deposits mainly consisted of Mo. The deposition rate of Mo was about ten times higher than that of the low-density discharge case. The hydrogen concentrations (H/Mo) retained in the co-deposits were 0.06–0.17, which was much higher than that in bulk-Mo and almost equal to the low-density case. These results indicate that as long as the co-deposition layers are continuously formed, strong wall pumping in TRIAM-1M is maintained during the discharges.

1. Introduction

Recycling and wall pumping properties are crucial issues for density control of a steady state plasma operation in thermonuclear fusion devices. In the all-metal machine TRIAM-1M, strong continuous wall pumping and temporal reduction of the wall pumping capability have been reported [1]. Such phenomenon may be strongly correlated with the formation of the co-deposition layer. Co-deposition layer is formed by re-deposit of the impurities emitted from the surface of in-vessel components due to the plasma wall interaction. In our previous study, a large amount of retained hydrogen were detected in a co-deposition layer formed under low plasma density ($\tilde{n}_e \sim 10^{18}$ m^{-3}) long pulse (4320 s) LHCD discharge in TRIAM-1M [2]. The plasma density of this experiment seems too low to perceive the phenomena in reactors. In case of ITER, for example, the expected density is $\sim 10^{20}$ m^{-3} [3]. Therefore, we will need to study the wall pumping properties under high density

* Corresponding author. Tel.: +81 92 583 7719; fax: +81 92 583 7690.
E-mail address: tokitani@riam.kyushu-u.ac.jp (M. Tokitani).

0022-3115/$ - see front matter © 2007 Elsevier B.V. All rights reserved.
doi:10.1016/j.jnucmat.2007.04.010

plasmas. In case of TRIAM-1M, the reported wall pumping rate for the high density ($\tilde{n}_e \sim 10^{19}$ m^{-3}) discharge was about ten times higher than that of the low density ($\tilde{n}_e \sim 10^{18}$ m^{-3}) discharge [1]. From the previous studies, we can consider that such a difference of wall pumping rate is strongly correlated with the properties of deposition, such as deposition rate and microstructure, and incidence flux of charge exchange (CX) neutral hydrogen atoms to the surface of the wall [4–7]. In the present work, therefore, hydrogen retention in co-deposits under high density plasma discharges in TRIAM-1M were studied by means of ion beam analysis technique and many other analytical techniques such as transmission electron microscopy (TEM).

2. Experimental procedures

TRIAM-1M ($R_{major} = 0.8$ m, $a \times b = 0.12$ m $\times$ 0.18 m) is a medium-sized tokamak machine with superconducting toroidal magnetic coils. The vacuum vessel is made of stainless steels. Limiters and divertors are made of Mo. To examine the effects of the co-deposits on the wall pumping, material probe experiments were carried out by using the surface probe system attached to TRIAM-1M. Fig. 1 shows the schematic view of the experimental set up of this study. Specimens of bulk-Si, -W and pre-thinned-SUS316L, -Mo were mounted on the probe head at the plasma facing side (P-side), electron drift side (E-side) and slope-area (S-area). In order to avoid the ions moving along the magnetic line of force, pre-thinned-Mo specimens were placed at the bottom of the holes with depths of 6 mm and diameter of 3 mm at the P-side (see Fig. 1). The probe head was inserted in the scrape-off layer (SOL) and exposed to 186 shots of high density 8.2 GHz LHCD hydrogen discharges with limiter configuration. The total discharge time was 407 s. Typical plasma parameters were $I_p \sim 30$ kA, $\tilde{n}_e \sim 1 \times 10^{19}$ m^{-3}, $T_i \sim 0.8$ keV. The temperature of the probe head during discharges did not change much and was kept at about room temperature. The specimens on the P-side were located 5 mm behind the poloidal limiter surface, as shown in Fig. 1.

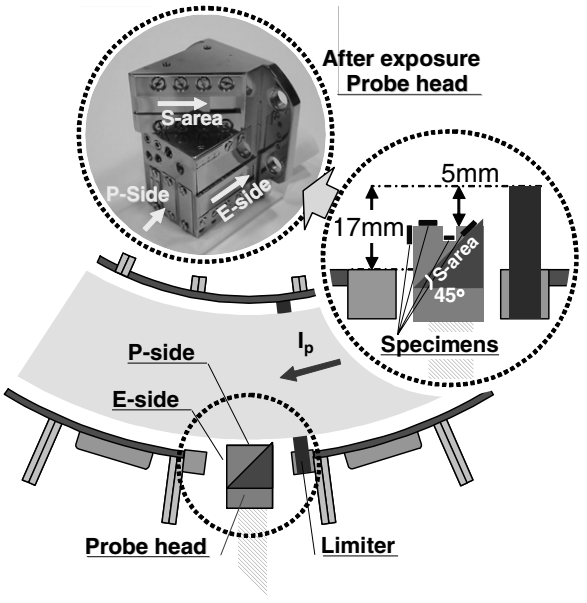

Fig. 1. Schematic view of the experimental set up.

After the exposure, thickness and chemical composition of co-deposition layers were analyzed quantitatively by using the simultaneous measurement technique of Rutherford back scattering spectrometry (RBS) and elastic recoil detection (ERD), respectively, with a ^{4}He analyzing beam of 2.8 MeV. The incident angle of analyzing beam was 72° to the surface normal of the specimen. The back scattered ^{4}He atoms were detected with the RBS detector placed at an angle of 170° to the incidence direction. The recoiled hydrogen atoms were detected by the ERD detector at the angle of 30° to the analyzing beam direction. An Al film of 12 μm thick was installed in front of the ERD detector to absorb the scattered He ions from the specimen surface. Microstructural modifications were observed by TEM. Surface morphology and chemical composition were also analyzed.

3. Results and discussion

3.1. Co-deposited layer and its deposition rate

Co-deposited layers mainly consisting of Mo were detected by the RBS on all the specimens exposed to the plasma. The thickness of the deposited Mo on W and Si specimens placed at the P-side (W), E-side (Si) and S-area (Si), are plotted in Fig. 2 against the distance from the limiter surface. In the area above 5.5 mm, the thickness of Mo at the E-side and the S-area gradually decreased with increasing distance from the plasma. The deposition rate at the S-area is much higher than that of the E-side one. For example, the deposition rate at 8 mm on the E-side and the S-area were 1.8×10^{18} Mo/m^2 s and 4.6×10^{18} Mo/m^2 s, respectively. The deposition rate at the P-side was also

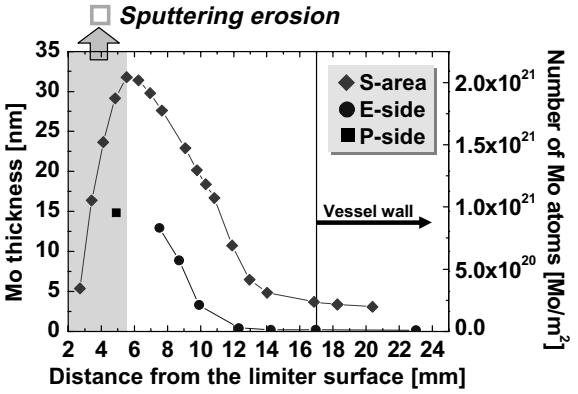

Fig. 2. Thickness distribution of the deposited Mo.

higher than that of E-side. These results indicate that the influx of the impurities has a strong directional dependence.

In contrast to the results at >5.5 mm, the thickness of Mo at the S-area decreased with decreasing distance (hatched area in Fig. 2). It is expected that strong sputtering erosion due to the ionized drift particles occurs in the area close to the plasma. Additionally, blistering and flaking were observed on the surface of the deposition layer by scanning electron microscopy (SEM). It is considered that these are the main reasons for the reduction of the net deposition rate at less than 5.5 mm.

3.2. Comparison with the low density case

The deposition rate at the P-side and E-side for high density (this work) and low density (previous work [2]) cases are compared in Fig. 3. It is remarkable that the deposition rate at the P-side of the high density case is about 36 times higher than that of the low density case. The deposition rate at the E-side was fitted by the following equation where exponential decay along radial direction of the plasma was assumed.

$$y = A\mathrm{e}^{-x/\lambda}.$$

Here A, x, λ, and y are a constant, the distance from limiter surface, the radial decay length of deposited Mo flux and its deposition rate, respectively. The best fitted constants (A) are 8.8×10^{19} for the high density case and 5.1×10^{18} for the low density case, and decay lengths (λ) is 2.0 mm (high density) and 1.9 mm (low density). These results indicate that the net deposition rate at the E-side for the high density case is about 17 times higher than that for the low density case, but the radial distribution does not depend on the density of the plasma. The radial decay length obtained in the present work is quite similar to that of JET ($\lambda = 2.0$ mm) [8].

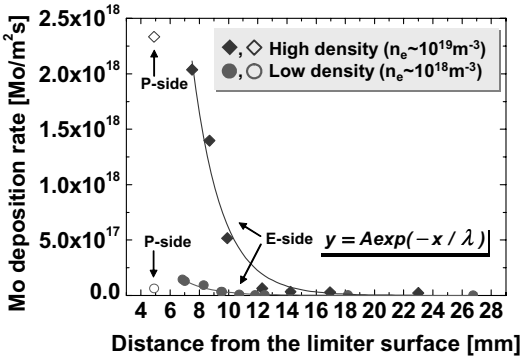

Fig. 3. Comparison of the deposition rate at the P-side and E-side on high density (this work) and low density (our previous work [2]) cases.

3.3. Microstructure observation

TEM micrographs and electron diffraction patterns of the specimens (SUS316L and Mo (in the hole)) exposed to the plasma are shown in Fig. 4. Fig. 4(a) shows the dark field TEM images of the deposits formed on the specimens (SUS316L) at the P-side and E-side. The images were obtained from a part of the first Debye ring which originated from the deposited materials. Only the crystal grains satisfying the Bragg condition have a bright image. For both cases, the deposits consisted of normal bcc polycrystals with lattice constant of 0.35 nm the grain size of about 10–20 nm in diameter. As reported in Ref. [4], residual oxygen strongly affects the structure of the deposits. If the deposition rate of Mo is relatively low, co-deposited oxygen suppresses free migration and crystallization of the deposited Mo atoms on the surface, and results in the formation of fcc polycrystals with very fine grains (1–2 nm). Such deposits are typically observed in the low density discharge [2]. It is considered that the deposited layers formed under the high density plasma discharges become bcc crystallines with rather large size because the deposition rate of Mo is sufficiently high and the role of oxygen is relatively minor.

Fig. 4(b) shows dark field TEM images obtained from a diffraction spot originated from the substrate material. The bright images indicate the defects, mainly dislocation loops, formed in the substrate

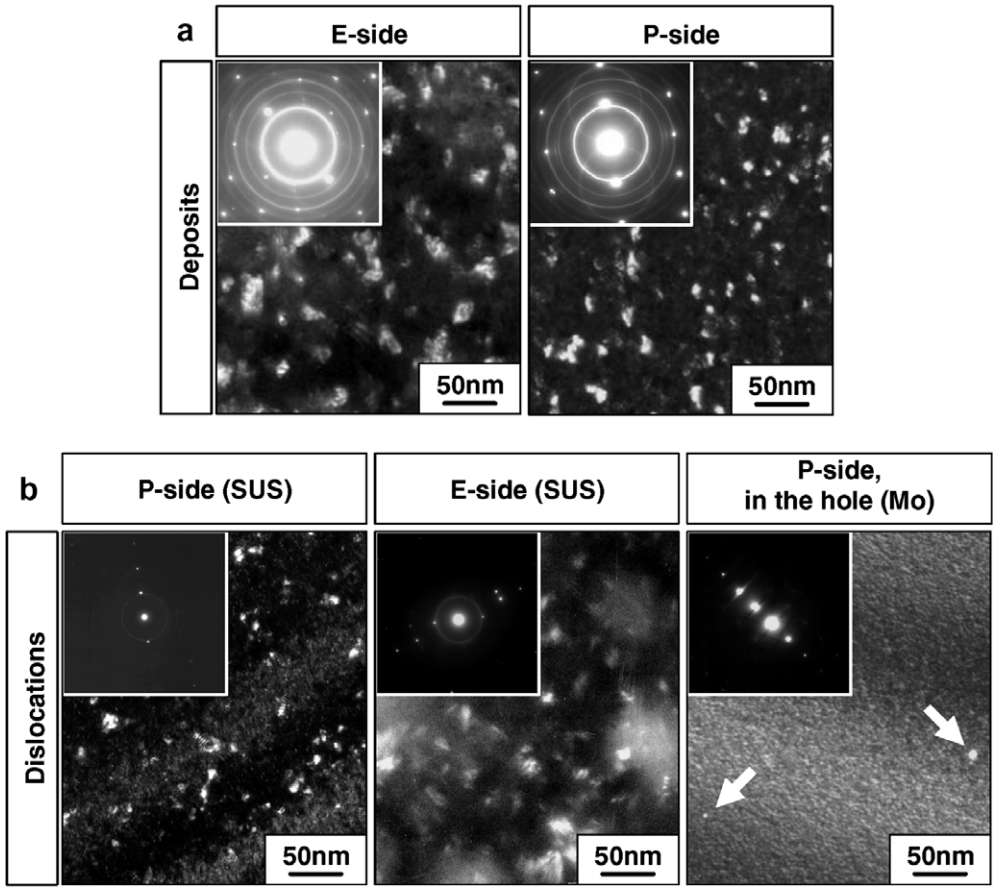

Fig. 4. Microstructure of SUS316L and Mo (in the hole) specimens. (a) shows the dark field images of the deposits on SUS316L specimens at the P-side and E-side and (b) shows the dark field images of the defects, mainly dislocation loops formed in the substrate specimen at the E-side and P-side, and Mo specimen placed in the hole at the P-side.

materials. Formation of defects in the Mo specimen placed in the hole at the P-side indicates that CX-neutrals contribute to the damage. Since the threshold energies of hydrogen for displacement damage in SUS316L and Mo are about 0.36 keV and 0.85 keV, respectively, formation of the defects indicates the existence of high energy incident particles on the wall surface. It is expected that the CX-neutrals with rather high energy are incorporated into the materials directly and contribute to the wall pumping.

3.4. Wall pumping effects by co-deposition layer

In Fig. 5 the amount of retained hydrogen in co-deposition layers on Si and W specimens is plotted as a function of the thickness of the deposits. These data were obtained by subtracting the background by comparing with the data of the un-irradiated specimens.

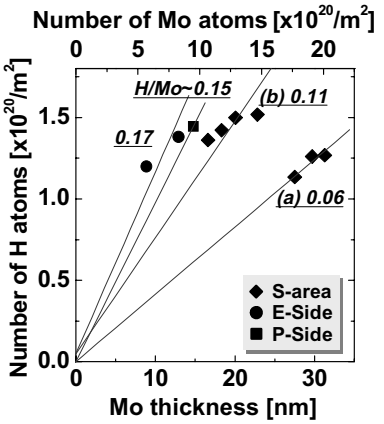

Fig. 5. Amount of retained hydrogen in the deposits on Si (at the E-side and S-area) and W (P-side) specimens as a function of the thickness of the deposits.

The evaluated hydrogen concentrations (H/Mo) at the P-side and E-side were 0.15 and 0.17,

respectively. In the S-area, the H/Mo is not simple; the hydrogen concentrations (H/Mo) must be roughly divided into (a) thick and (b) thin deposition areas. The data of (a), 0.06, correspond to the medium range/area from the plasma (6–8 mm in Fig. 2) and the data of (b), 0.11, to the remote range/area from the plasma (9–11 mm in Fig. 2). It is considered that the rather low hydrogen concentration of (a) may be influenced by sputtering erosion. These values were much higher than bulk-Mo and almost equal to the low density discharge case [2]. Consequently, the hydrogen retention rate under high density discharges which was estimated from RBS and ERD measurements at the P-side, E-side, and S-area were 3.5×10^{17} H/m^2 s, 2.9×10^{17} H/m^2 s, and (a) 2.8×10^{17} H/m^2 s or (b) 3.4×10^{17} H/m^2 s, respectively. These values were about ten times higher than that of low density case [2]. On the other hand, the averaged wall pumping rate in a similar high density short pulse LHCD discharges in TRIAM-1M was evaluated at about 4.0×10^{17} H/m^2 s based on a global particle balance [1]. This value is quite similar to those estimated by the present work. Therefore, we can say that strong continuous wall pumping in TRIAM-1M is due to the retention of hydrogen in the co-deposited layer.

In Tore Supra, which uses carbon fiber composites (CFCs) for in-vessel components, the in-vessel gas inventory (wall pumping) does not show any sign of saturation after 4 min of deuterium discharge. In this case, it was known that the carbon co-depositions were contributed to the wall pumping of Tore Supra ($D/C = 0.4$) and the metallic surfaces were negligible deuterium sinks [9]. However, the present result shows that the wall pumping due to the co-deposition occurs not only in carbon machine but also in metal machine.

4. Summary

The hydrogen retentions in the co-deposition formed under high density plasma discharge in TRIAM-1M were studied by means of ion beam analysis, TEM and other several analytical techniques. In the case of high density discharge, the net deposition rate of Mo impurities was much higher than that of low density case. The deposits are polycrystals of about 10–20 nm in diameter and have normal bcc structure. The hydrogen retention rates in the deposits at the P-side, E-side, and S-area were 3.5×10^{17} H/m^2 s, 2.9×10^{17} H/m^2 s, and (a) 2.8×10^{17} H/m^2 s or (b) 3.4×10^{17} H/m^2 s, respectively. These values are about ten times higher than that of low density discharge [2] and sufficient to explain the higher wall pumping rate of high density discharges in TRIAM-1M. These results indicate that the co-deposition of metallic impurities play major role for the wall pumping even in the metal machine.

Acknowledgements

The authors would like to thank Professor K. Kakimoto of the Research Institute for Applied Mechanics, Kyushu University for providing the Si specimens. This work was performed under the inter-university cooperative research program of the Institute for Materials Research, Tohoku University. This research was partly supported by the Japan Society for the Promotion of Science and Grant-in-Aid of Scientific Research from Japan Ministry of Education, Culture, Sports, Science and Technology.

References

[1] M. Sakamoto, S. Itoh, K. Nakamura, H. Zushi, K. Hanada, E. Jotaki, Y.D. Pan, S. Kawasaki, N. Nakashima, Nucl. Fusion 42 (2002) 165.
[2] M. Miyamoto, M. Tokitani, K. Tokunaga, T. Fujiwara, N. Yoshida, M. Sakamoto, H. Zushi, S. Nagata, K. Ono, TRIAM Group, J. Nucl. Mater. 337–339 (2005) 436.
[3] V. Mukhovatov, M. Shimada, A.N. Chudnovskiy, A.E. Costley, Y. Gribov, G. Federici, O. Kardaun, A.S. Kukushkin, A. Polevoi, V.D. Pustovitov, Y. Shimomura, T. Sugie, M. Sugihara, G. Vayakis, Plasma Phys. Control. Fus. 45 (2003) A235.
[4] T. Hirai, T. Fujiwara, K. Tokunaga, N. Yoshida, A. Komori, O. Motojima, S. Itoh, TRIAM Group, J. Nucl. Mater. 283–287 (2000) 1177.
[5] T. Hirai, T. Fujiwara, K. Tokunaga, N. Yoshida, S. Itoh, TRIAM Group, J. Nucl. Mater. 290–293 (2001) 94.
[6] M. Miyamoto, T. Hirai, K. Tokunaga, T. Fujiwara, N. Yoshida, J. Nucl. Mater. 307–311 (2002) 710.
[7] M. Miyamoto, K. Tokunaga, T. Fujiwara, N. Yoshida, TRIAM Group, Y. Morimoto, T. Sugiyama, K. Okuno, J. Nucl. Mater. 313–316 (2003) 82.
[8] G.M. McCracken, J. Ehrenberg, P.E. Stott, R. Behrisch, L. de Kock, J. Nucl. Mater. 145–147 (1987) 621.
[9] J. Jacquinot on behalf of the EURATOM-CEA Association, Nucl. Fusion 43 (2003) 1583–1599.